The solubility of hydrogen in the A-15 compounds V_3Ga and Ti_3Ir

1990 J. Phys.: Condens. Matter 2 6929

(http://iopscience.iop.org/0953-8984/2/33/005)

J. Phys.: Condens. Matter 2 (1990) 6929–6938. Printed in the UK

The solubility of hydrogen in the A-15 compounds V_3Ga and Ti_3Ir

M Schlereth and H Wipf
Institut für Festkörperphysik, Technische Hochschule Darmstadt, Hochschulstrasse 6, D-6100 Darmstadt, Federal Republic of Germany

Received 22 March 1990

Abstract. The solution behaviour of hydrogen in the A-15 compounds V_3Ga and Ti_3Ir was studied by hydrogen absorption and x-ray diffraction measurements. It was found that the presence of the hydrogen did not change the structure of the A-15 host crystals. The lattice parameter, the partial enthalpy of solution and the partial entropy of solution were determined for both compounds investigated as a function of the hydrogen content.

1. Introduction

This paper reports on the results of a study in which we investigated the solution behaviour of hydrogen in the two A-15 compounds V_3Ga and Ti_3Ir. A-15 compounds are an important class of materials comprising, in particular, several superconductors of high technological interest (see [1] for a review article). Both compounds investigated are superconductors with transition temperatures of ~15 K (V_3Ga) [1–3] and ~ 4 K (Ti_3Ir) [1, 4]. Our study was performed using two different experimental procedures. We carried out hydrogen absorption measurements from which we derived solubility isotherms in the range between room temperature and 600 °C (for V_3Ga) or 800 °C (for Ti_3Ir). The results allowed the determination of the partial enthalpy and the partial entropy of solution as a function of the hydrogen content of the investigated compounds. Secondly, we performed x-ray diffraction measurements which demonstrated that the cubic A-15 structure of the host crystals did not change upon hydrogen doping. We determined further, at room temperature, the lattice parameter of the respective crystals as a function of the hydrogen content.

Previous studies on the effects of hydrogen in A-15 compounds were chiefly devoted to its impact on the superconducting transition temperature. Experiments carried out on Ti_3AuH_x, Ti_3SbH_x, V_3GaH_x, V_3GeH_x, V_3SiH_x, Nb_3AlH_x, Nb_3GeH_x and Nb_3SnH_x established a continuous depression of the transition temperature with rising hydrogen content, with the exception of a few cases where this temperature was found to increase slightly at low hydrogen concentrations x [5–18]. The only detailed study on the solubility behaviour of hydrogen in an A-15 compound was performed on the system Ti_3SbH_x [19]. The diffusion of hydrogen in Nb_3SnH_x has been investigated by internal friction measurements [20]. Structural studies showed that, in general, the A-15 lattice structure remains unchanged even at high hydrogen concentrations x, and that the lattice parameter increases with rising x [6–8, 11, 15, 19, 20]. This trend is confirmed by the

0953-8984/90/336929 + 10 $03.50

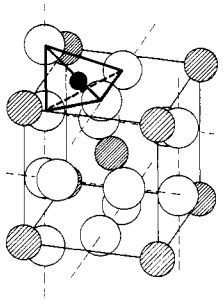

Figure 1. Cubic unit cell of the A-15 compounds V_3Ga and Ti_3Ir. The small, full circle indicates the position of a tetrahedral interstitial site.

results of the present study. Neutron diffraction measurements carried out on Nb_3SnH_x demonstrated that the dissolved hydrogen in this compound is located on tetrahedral interstitial sites [8]. As a consequence of this result, it was generally assumed that hydrogen occupies tetrahedral interstitial sites also in other A-15 compounds. Figure 1 shows the position of such a tetrahedral site for the A-15 compounds V_3Ga and Ti_3Ir investigated in the present study. Since there are three tetrahedral sites per Nb_3Sn (or V_3Ga, etc) formula unit, an occupation of these sites limits the maximum hydrogen concentration to $x = 3$. As a surprising result of the present study it will be seen that—for an unchanged A-15 host lattice—the maximum hydrogen concentration found for Ti_3IrH_x exceeds $x = 3$ so that the hydrogen at least in this system does not, or not exclusively, occupy tetrahedral interstitial sites.

2. Experimental procedure

The samples of the two A-15 compounds investigated V_3Ga (typically 2.5 g) and Ti_3Ir (~9 g) were prepared from their metallic constituents by repeated melting processes (up to 30 times) in a water-cooled copper crucible located in an induction furnace (~600 mbar Ar atmosphere). The samples were rotated between the individual melting processes in order to improve homogenisation. In the case of V_3Ga, the high Ga vapour pressure resulted in noticeable evaporation losses which could reliably be monitored from the continuous weight decrease of the individual samples. To compensate for these losses, the amount of Ga initially added was kept above its stoichiometric ratio, and the melting processes were terminated after the correct stoichiometry, as determined by weight, was reached. The Ti_3Ir samples were, after the last melting process, annealed for homogenisation at ~1450 °C for about half an hour and subsequently slowly cooled [21].

The hydrogen solubilities were determined from pressure–composition isotherms taken in an UHV system. The investigated sample was in a temperature-controlled chamber (about 200 cm^2) with a temperature stability of 0.3 °C and an absolute temperature accuracy ranging from ±1 °C at room temperature up to ±20 °C at the highest temperature investigated (800 °C). The sample chamber could be connected to calibrated standard volumes. The hydrogen gas, which was admitted to the system, was purified in a palladium permeation cell, and the hydrogen gas pressures in the sample chamber and in the standard volumes could be measured by sensitive differential membrane manometers (pressures up to ~5 bar). The measurement of the hydrogen gas pressure allowed, with the help of the standard volumes, the precise determination of the total amount of hydrogen gas in the system and, therefore, the hydrogen concentration of the sample also.

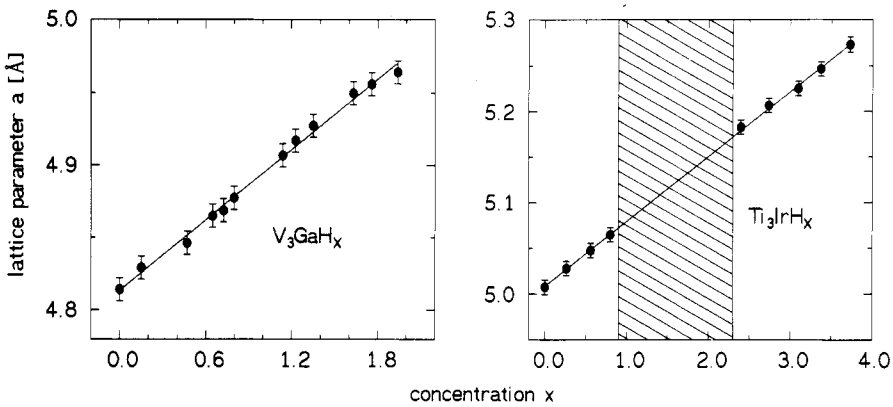

Figure 2. Lattice parameter, a, of V_3GaH_x (left hand side) and Ti_3IrH_x (right hand side) versus hydrogen concentration, x. The hatched area indicates the concentration range $0.9 \leq x \leq 2.3$ of the miscibility gap for the Ti_3IrH_x system.

The x-ray studies were performed at room temperature with a conventional powder diffractometer (Cu Kα radiation). The hydrogen doping of the powder samples investigated by x-ray diffraction was carried out in the UHV system that was used for the solubility measurements. The hydrogen concentration of these samples was determined from the absorption data and, additionally, from a heat extraction analysis in a separate (calibrated) vacuum system (accuracy 1% of the value of the concentration x).

3. Experimental results and discussion

3.1. X-ray diffraction measurements on V_3GaH_x and Ti_3IrH_x

The A-15 structure of all the V_3Ga and Ti_3Ir samples prepared was established by x-ray diffraction prior to the actual hydrogen absorption studies. The lattice parameter found at room temperature was 4.814 Å for V_3Ga and 5.007 Å for Ti_3Ir. These values are in agreement with those reported in the literature [3, 4, 22].

The diffraction measurements carried out on the hydrogen-doped samples demonstrated in all cases an A-15 structure for the V_3Ga or Ti_3Ir host lattice. The left hand side of figure 2 shows our results for the (cubic) lattice parameter a of V_3GaH_x as a function of the hydrogen concentration x. In the concentration range investigated up to $x \simeq 2.0$, the lattice parameter of V_3GaH_x exhibits a linear increase with x which is quantitatively described by $da/dx = (7.75 \pm 0.3) \times 10^{-2}$ Å. This concentration dependence agrees essentially with that reported from two previous studies [11, 14] although we do not find any evidence for a miscibility gap as suggested in [11] in the range $0.4 \leq x \leq 1.0$.

The concentration dependence of the lattice parameter a determined from our Ti_3IrH_x powder samples is presented in the right hand side of figure 2. The measurements established the existence of a miscibility gap in the concentration range between $x = 0.9$ and $x = 2.3$. In this concentration range, the diffraction data demonstrated the coexistence of two phases with lattice parameters that corresponded to those for hydrogen concentrations at the lower and upper limit of the miscibility gap. It will be seen

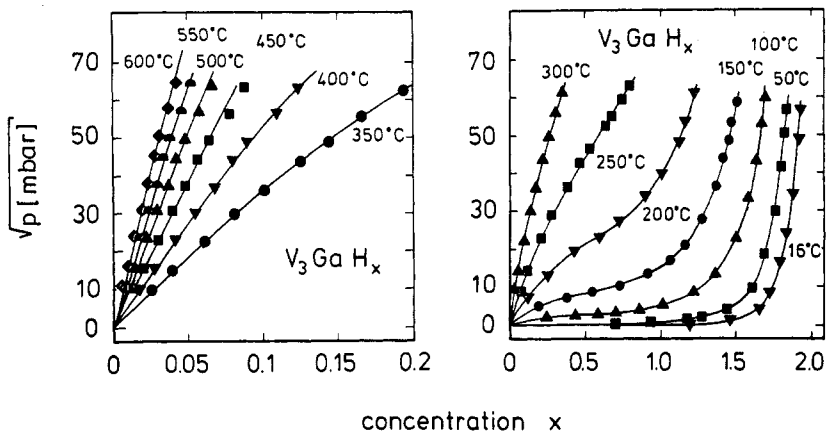

Figure 3. Hydrogen absorption isotherms of the $V_3 GaH_x$ system for small (left hand side) and high (right hand side) hydrogen concentrations. In both plots, the square root of the hydrogen gas pressure p is plotted versus the hydrogen concentration x. The full curves are guides to the eye.

later that our solubility data do indicate the existence of a miscibility gap for the Ti_3IrH_x system as well.

The lattice parameter data for Ti_3IrH_x extend up to a maximum hydrogen concentration $x = 3.8$. This maximum concentration is incompatible with a sole occupation of tetrahedral interstitial sites since there are only three such sites per Ti_3Ir formula unit. Our results demonstrate, therefore, that the dissolved hydrogen in Ti_3Ir does not—or not exclusively—occupy tetrahedral interstitial sites. A reliable determination of the actual interstitial positions of the hydrogen in Ti_3Ir would, however, require neutron diffraction measurements since x-ray data do not provide such structural information for hydrogen isotopes.

The right hand side of figure 2 shows, except for the miscibility gap, a linear concentration dependence of the lattice parameter a of Ti_3IrH_x. The concentration dependence is described by $da/dx = (7.2 \pm 0.3) \times 10^{-2}$ Å. Finally, it seems interesting to note that the hydrogen-induced lattice expansion for both systems investigated, V_3GaH_x and Ti_3IrH_x, corresponds to a volume increase of $\Delta V = 2.7$ Å^3 per absorbed hydrogen atom which agrees well with the very general value of $\Delta V \simeq 2.9$ Å^3 found in a large number of metallic hosts [23].

3.2. Solubility data for V_3GaH_x

The two plots of figure 3 represent, as the result of our solubility measurements on V_3GaH_x, absorption isotherms taken in the temperature range between 16 and 600 °C. Note that the concentration ranges in the abscissae of the two plots of figure 3 are different in order to yield a better concentration resolution for the high-temperature data in the left hand side plot. The data demonstrate an exothermic solution behaviour since, for a given hydrogen gas pressure p, the hydrogen concentration x increases with falling temperature.

The results depicted in figure 3 allow the determination of the partial enthalpy of solution $\Delta h = h_H - \frac{1}{2}h^{(0)}_{H_2}$ and of the partial entropy of solution $\Delta s = s_H - \frac{1}{2}s^{(0)}_{H_2}$ (see [24–

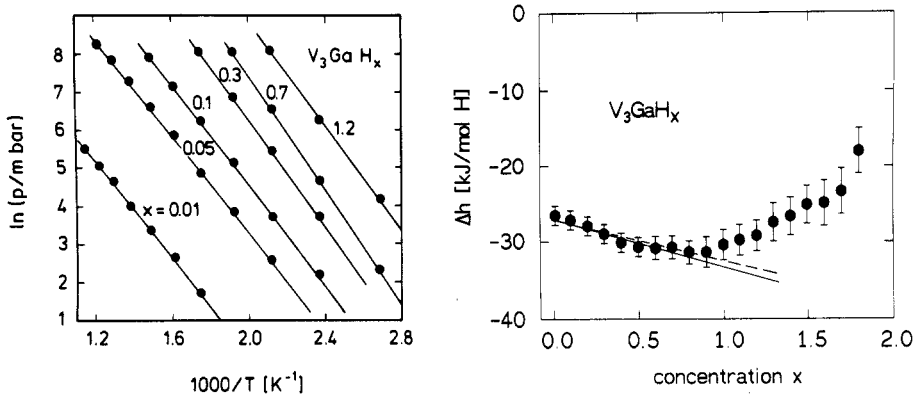

Figure 4. Partial enthalpy of solution Δh for the V_3GaH_x system. The left hand side of the figure shows a van't Hoff plot in which the logarithm of the hydrogen gas pressure p is, for six different values of x, plotted versus the reciprocal temperature T. The right hand side shows the results for Δh versus x. Within experimental accuracy, Δh was found to be temperature independent. The meaning of the full and the broken line is explained in the text.

26] and references therein). In the preceding expressions, h_H is the partial enthalpy and s_H is the partial entropy of a dissolved hydrogen atom, whereas $h^{(0)}_{H_2}$ and $s^{(0)}_{H_2}$ are the enthalpy and the entropy of a hydrogen molecule for a standard reference pressure $p_0 = 1$ atm $= 1.01325$ bar. The partial enthalpy of solution Δh can be determined experimentally with the help of the van't Hoff equation [24–26]:

$$\Delta h = (R/2)\,\partial \ln(p)/\partial(1/T)|_x \tag{1}$$

where the subscript x denotes a differentiation with a constant concentration x (R is the molar gas constant, and T is the temperature). In a similar way, the partial entropy of solution can be obtained from the relation

$$\Delta s = -(R/2)\,\partial \ln(p/p_0)/\partial T|_x. \tag{2}$$

The left hand side of figure 4 presents a van't Hoff plot for V_3GaH_x from the results of our solubility data. The figure shows, for six hydrogen concentrations x, the logarithm of the hydrogen gas pressure p plotted versus the reciprocal temperature. The slope of the curves connecting the data points for a given concentration yields, according to (1), the value of the partial enthalpy of solution Δh for this concentration. It can be seen from the left hand side of figure 4 that, for a given curve, the slope does not vary with temperature, which means that Δh is temperature independent at least within its experimental accuracy.

The right hand side of figure 4 presents our results for the partial enthalpy of solution Δh for V_3GaH_x versus hydrogen concentration x. The data demonstrate an initial decrease of Δh with rising x which, above $x \simeq 0.8$, is then followed by a continuous increase. The initial decrease can be explained as a result of an elastic interaction between the hydrogen interstitials [27]. Such an interaction yields, within an elasticity–theoretical approximation, a concentration dependence of Δh given by [27]

$$\mathrm{d}\Delta h/\mathrm{d}x = -[(\gamma_E - 1)/\gamma_E](2/a^3)(P^2/B) \tag{3}$$

where $3P$ is the trace of the double force tensor of the dissolved hydrogen, and a, γ_E and

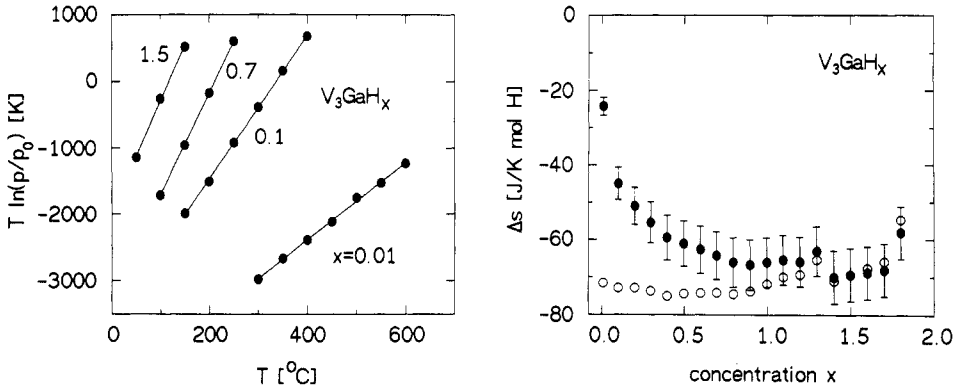

Figure 5. Partial entropy of solution Δs for the V_3GaH_x system. The left hand side of the figure shows, for four values of x, the quantity $T\ln(p/p_0)$ versus temperature T, where p is the hydrogen gas pressure and $p_0 = 1.01325$ bar. The full data points on the right hand plot shows the results for Δs as a function of x. Within experimental accuracy, Δs was found to be temperature independent. The open data points indicate the non-configurational part Δs^{nc} of Δs derived under the assumption of a maximum concentration $x_{max} = 3$ (this corresponds to an occupation of tetrahedral interstitial sites).

B are the (cubic) lattice parameter, the Eshelby factor and the bulk modulus of V_3Ga, respectively. For an isotropic system, the Eshelby factor is defined as $\gamma_E = (3B + 4\mu)/(3B)$ where μ is the shear modulus (note that the present definition for γ_E corresponds to that in [27] and [28] rather than to the different one given, e.g., in [29]). The above equation considers also the fact that, for a given x, the number of hydrogen interstitials per unit volume is $2x/a^3$. The trace $3P$ of the double force tensor is related to the hydrogen-induced lattice expansion according to the relation [23, 27, 29]

$$P = (3Ba^2/2)(da/dx) \tag{4}$$

so that the concentration dependence of the partial enthalpy of solution can be written as

$$d\Delta h/dx = -[(\gamma_E - 1)/\gamma_E](9Ba/2)(da/dx)^2. \tag{5}$$

The calculation of the bulk modulus B and the Eshelby factor γ_E requires the knowledge of the three elastic moduli of V_3Ga for which we did not find sufficient data in the literature. We made, therefore, an estimate for $d\Delta h/dx$ according to (5) with the help of the room temperature elastic moduli of the related compounds V_3Ge and V_3Si [30, 31]. The isotropic shear modulus μ, which is required for the calculation of the Eshelby factor, was assumed to be the average between the shear moduli resulting from the two averaging procedures of Voigt and Reuss [29]. The concentration dependence of the partial enthalpy of solution Δh, following from the above estimate for the elastic interaction, is indicated in the right hand side of figure 4 by a full and a broken line which represent the results obtained from the elastic moduli of V_3Si and V_3Ge, respectively. These results agree well with the experimentally observed initial decrease of Δh which demonstrates that the elastic interaction is likely to provide the dominant contribution to the concentration dependence of Δh for low hydrogen concentrations x.

We consider now the partial entropy of solution, Δs. The left hand side of figure 5 shows, for four different concentrations x, the quantity $T\ln(p/p_0)$ versus temperature

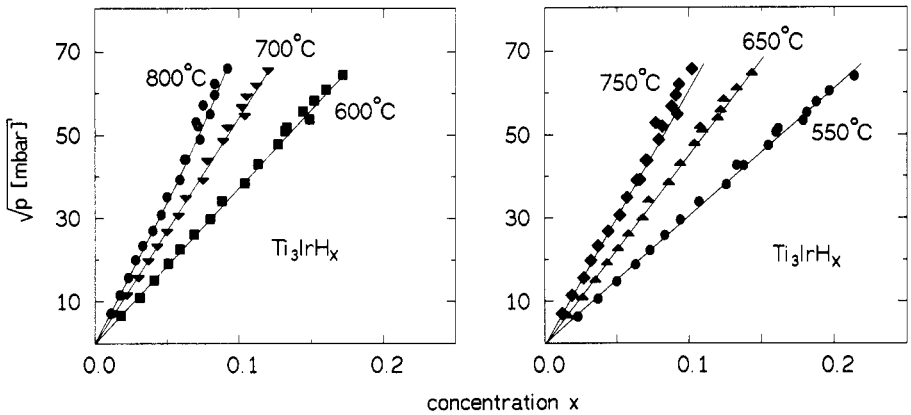

Figure 6. Hydrogen absorption isotherms of the Ti_3IrH_x system in the temperature range between 550 and 800 °C. The data are presented in two plots in order to allow better data resolution. The full lines are guides to the eye.

T. The entropy of solution Δs is, according to (2), obtained from the slope of the curves through the data points for a given x. Similarly as in the case of Δh, we can see from figure 5 that Δs does not, within experimental accuracy, noticeably depend on temperature. The full data points in the right hand side of figure 5 are our results for the partial entropy of solution Δs versus hydrogen concentration x. The data exhibit a divergency for $x \rightarrow 0$ which is due to the configurational part of the partial entropy s_H of the dissolved hydrogen. In order to eliminate this divergency, it is a common procedure to split the partial entropy of solution Δs according to [24–26]

$$\Delta s = \Delta s^{nc} - R \ln[x/(x_{max} - x)] \tag{6}$$

where the second term of the right hand side of the above equation is the configurational part of the partial entropy s_H of the dissolved hydrogen. The quantity x_{max} is the maximum hydrogen concentration as given by the total number of available interstitial sites that are occupied by hydrogen. For tetrahedral sites in an A-15 structure, this maximum concentration is $x_{max} = 3$. The term Δ^{nc} in (6) is the non-configurational part of the partial entropy of solution Δs which can be calculated from Δs for a given value of x_{max}. The open data points in the right hand side of figure 5 show our results for Δs^{nc} derived under the assumption of an occupation of tetrahedral sites. It can be seen that Δs^{nc} is essentially independent of x which demonstrates that the concentration dependence of the partial entropy of solution Δs is mainly due to the configurational part of the partial entropy of the dissolved hydrogen.

3.3. Solubility data for Ti_3IrH_x

The hydrogen absorption isotherms measured for the system Ti_3IrH_x are presented in figures 6 and 7. Figure 6 shows the results obtained in the temperature range between 550 and 800 °C in two plots in order to allow a better discrimination between the data for different temperatures. The isotherms measured between room temperature and

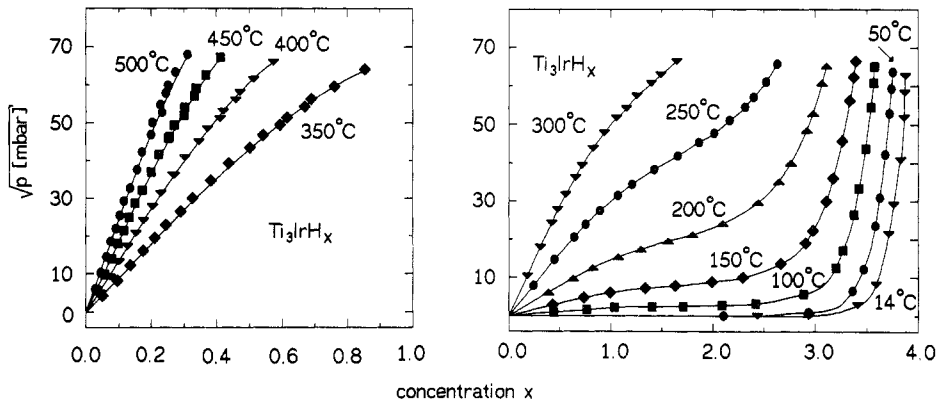

Figure 7. Hydrogen absorption isotherms of the Ti_3IrH_x system between room temperature and 500 °C. The data are presented in two plots in order to allow better data resolution. The full curves are guides to the eye.

500 °C are found in the two plots of figure 7 which, again in order to allow a better data resolution, extend over different concentration and temperature regimes.

The hydrogen absorption in the Ti_3IrH_x system is, similarly as in the case of V_3GaH_x, exothermic since the equilibrium hydrogen gas pressure decreases with falling temperature for a given concentration x. The absorption isotherms at 100 °C (and below) are very flat in the concentration range $0.9 \leq x \leq 2.3$ thus indicating the occurrence of the miscibility gap which was definitely established in our x-ray diffraction measurements. The data in the right hand side of figure 7 demonstrate further that the maximum hydrogen concentration reached in our experiments for the Ti_3IrH_x system was $x = 3.9$. This value exceeds by far the maximum concentration $x = 3$ compatible with a sole occupation of tetrahedral interstitial sites. The solubility data confirm, therefore, the conclusion from our diffraction measurements that the dissolved hydrogen in Ti_3IrH_x does not—or not exclusively—occupy tetrahedral interstitial sites. It should be mentioned here that the maximum hydrogen concentrations x achieved for both systems investigated in the present study, V_3GaH_x and Ti_3IrH_x, were limited by the highest hydrogen gas pressure of ~5 bar that was tolerable in our vacuum system. The fact that the concentrations observed in the V_3GaH_x system were below $x = 2$ is, accordingly, no proof at all that the hydrogen in this system actually does not occupy any sites other than tetrahedral sites.

We determined from our absorption data in figures 6 and 7 the partial enthalpy of solution Δh and the partial entropy of solution Δs for the Ti_3IrH_x system by the same procedure we applied in the preceding section. Both quantities were found to be temperature independent within experimental accuracy. The results for Δh and Δs are presented in figure 8. The left hand side of this figure shows the partial enthalpy of solution Δh as a function of the hydrogen concentration x. The data indicate (as in the V_3GaH_x system) an initial decrease of Δh with rising x followed, above $x \simeq 3$, by an increase up to the maximum concentration investigated, $x = 3.9$. A comparison with figure 4 shows also that the values of Δh are nearly identical for the two systems investigated, V_3GaH_x and Ti_3IrH_x.

The right hand side of figure 8 represents the partial entropy of solution Δs versus x. The data indicate the divergency of this quantity for $x \rightarrow 0$, and they demonstrate that

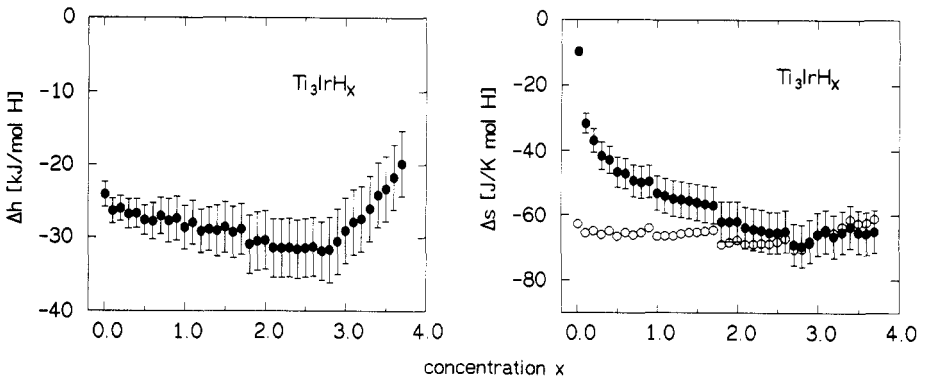

Figure 8. Partial enthalpy of solution Δh and partial entropy of solution Δs for the Ti_3IrH_x system. The left hand side of the figure shows Δh as a function of x. The full data points in the right hand plot are Δs versus x. The open data points indicate the non-configurational part Δs^{nc} of Δs derived under the arbitrary assumption of a maximum concentration $x_{max} = 6$.

the size of Δs is again very similar to that observed for the V_3GaH_x system. The open data points in the right hand side of figure 8 represent values for the non-configurational part Δs^{nc} of the partial entropy of solution Δs. It is obvious that Δs^{nc} cannot be derived from Δs under the assumption of hydrogen occupation of tetrahedral interstitial sites because the concentration range of the Ti_3IrH_x measurements exceeds the value $x = 3$. Since we do not know which interstitial site or sites are actually occupied, we arbitrarily presupposed a maximum hydrogen concentration $x_{max} = 6$ in order to calculate, according to (6), the data for Δs^{nc} in figure 8. It can be seen that this presupposition eliminates the divergency for $x \rightarrow 0$ whereby, on the other hand, the true values of Δs^{nc} as obtained for the (unknown) correct x_{max} differ from those presented in figure 8 essentially only by a constant as long as $x \ll x_{max}$.

4. Conclusions

We carried out hydrogen absorption and x-ray diffraction measurements on the two systems V_3GaH_x and Ti_3IrH_x. From the diffraction measurements, we determined (with the exception of a miscibility gap for Ti_3IrH_x) the lattice parameter of both systems investigated as a function of the hydrogen content. The data demonstrated that the A-15 structure of the V_3Ga and Ti_3Ir host crystals did not change upon hydrogen doping. This result is supported by the absorption measurements which revealed a completely reversible solubility behaviour in the entire temperature and hydrogen concentation range investigated. We exclude, therefore, a decomposition of the A-15 host crystals. A surprising result of our study was the maximum hydrogen concentration $x = 3.9$ observed in the Ti_3IrH_x system. This fact demonstrates that the dissolved hydrogen in Ti_3IrH_x does not—or not exclusively—occupy tetrahedral interstitial sites as reported from a neutron diffraction study on the related A-15 system Nb_3SnH_x [8]. Finally, we determined from our measured absorption isotherms the partial enthalpy of solution and the partial entropy of solution for both systems investigated as a function of the hydrogen concentration. For both systems, the results for the partial enthalpy of solution

are in the range between -20 and -30 kJ mol^{-1} H which is a factor of two smaller than the only previously reported value of the partial enthalpy of solution for hydrogen absorption in an A-15 host lattice (Ti_3SbH_x) [19].

Acknowledgment

This work was financially supported by the Bundesministerium für Forschung und Technologie.

References

[1] Muller J 1980 *Rep. Prog. Phys.* **43** 641
[2] van Winkel A and Bakker H 1985 *J. Phys. F: Met. Phys.* **15** 1565
[3] Ramakrishnan S, Nigam A K and Chandra G 1986 *Phys. Rev.* B **34** 6166
[4] Ramakrishnan S and Chandra G 1988 *Phys. Rev.* B **38** 9245
[5] Vertrano J B, Guthrie G L and Kissinger H E 1967 *Phys. Lett.* **26A** 45
[6] Ziegler G 1968 *Helv. Phys. Acta* **41** 1267
[7] Sahm P R 1968 *Phys. Lett.* **26A** 459
[8] Vieland L J, Wicklund A W and White J G 1975 *Phys. Rev.* B **11** 3311
[9] Zwicker U and Böhm W 1978 *Z. Metallk.* **69** 600
[10] Lanford W A, Schmidt P H, Rowell J M, Poate J M, Dynes R C and Dernier P D 1978 *Appl. Phys. Lett.* **32** 339
[11] Huang S Z, Skoskiewiecz T, Chu C W and Smith J L 1980 *Phys. Rev.* B **22** 137
[12] Nölscher C, Müller P, Adrian H, Lehmann M and Saemann-Ischenko G 1981 *Z. Phys.* B **41** 291
[13] Alterovitz S A, Farell D E, Chandrasekhar B S, Haugland E J, Blue J W and Liu D C 1981 *Phys. Rev.* B **24** 90
[14] Cort B, Stewart G R, Huang S Z, Meng R L and Chu C W 1981 *Phys. Rev.* B **24** 5058
[15] Shamrai V, Bohmhammel K and Wolf G 1982 *Phys. Status Solidi* b **109** 511
[16] Rama Rao K V S, Sturm H, Elschner B and Weiss A 1983 *Phys. Lett.* **93A** 492
[17] Elton J and Oesterreicher H 1983 *J. Less-Common Met.* **90** L37
[18] Ivanov M A, Kobzenko G F, Litvin S E, Morozovskii A E, Nikitin B G, Pan V M and Shkola A A 1986 *Sov. Phys.–Solid State* **28** 1397
[19] Rama Rao K V S, Mrowietz M and Weiss A 1982 *Ber. Bunsenges. Phys. Chem.* **86** 1135
[20] Berry B S, Pritchet W C and Bussière J F 1983 *Scr. Metall.* **17** 327
[21] Junod A, Flukiger R and Muller J 1976 *J. Phys. Chem. Solids* **37** 27
[22] Villars P and Calvert L D 1985 *Pearson's Handbook of Crystallographic Data for Intermetallic Compounds* (Metals Park, OH: American Society for Metals)
[23] Peisl H 1978 *Hydrogen in Metals I* (*Springer Topics in Applied Physics 28*) ed G Alefeld and J Völkl (Berlin: Springer) p 53
[24] Mueller W M, Blackledge J P and Libowitz G G (ed) 1968 *Metal Hydrides* (New York: Academic)
[25] Griessen R and Riesterer T 1988 *Hydrogen in Intermetallic Compounds I* (*Springer Topics in Applied Physics 63*) ed L Schlapbach (Berlin: Springer) p 219
[26] Schmidt R, Schlereth M, Wipf H, Assmus W and Müllner M 1989 *J. Phys.: Condens. Matter* **1** 2473
[27] Alefeld G 1972 *Ber. Bunsenges. Phys. Chem.* **76** 746
[28] Eshelby J D 1956 *Solid State Physics* vol 3 (New York: Academic) p 79
[29] Leibfried G and Breuer N 1978 *Point Defects in Metals I* (*Springer Tracts in Modern Physics 81*) (Berlin: Springer)
[30] Testardi L R and Bateman T B 1967 *Phys. Rev.* **154** 402
[31] Testardi L R, Kunzler J E, Levinstein H J, Maita J P and Wernick J H 1971 *Phys. Rev.* B **3** 107